Oxidation of ZrB2–SiC: Influence of SiC Content on Solid and Liquid Oxide Phase Formation

Article *in* Journal of the American Ceramic Society · January 2009

Impact Factor: 2.61 · DOI: 10.1111/j.1551-2916.2008.02874.x

2 authors:

Sigrun Nanna Karlsdottir
University of Iceland
31 PUBLICATIONS **297** CITATIONS
SEE PROFILE

John W. Halloran
University of Michigan
255 PUBLICATIONS **4,594** CITATIONS
SEE PROFILE

journal

J. Am. Ceram. Soc., 92 [2] 481–486 (2009)
DOI: 10.1111/j.1551-2916.2008.02874.x

Oxidation of ZrB_2–SiC: Influence of SiC Content on Solid and Liquid Oxide Phase Formation

Sigrun N. Karlsdottir[†,‡] and John W. Halloran

Department of Materials Science and Engineering, University of Michigan, Ann Arbor, Michigan 48104

The effect of SiC concentration on the liquid and solid oxide phases formed during oxidation of ZrB_2–SiC composites is investigated. Oxide-scale features called convection cells are formed from liquid and solid oxide reaction products upon oxidation of the ZrB_2–SiC composites. These convection cells form in the outermost borosilicate oxide film of the oxide scale formed on the ZrB_2–SiC during oxidation at high temperatures ($\geq$ 1500°C). In this study, three ZrB_2–SiC composites with different amounts of SiC were tested at 1550°C for various durations of time to study the effect of the SiC concentration particularly on the formation of the convection cell features. A calculated ternary phase diagram of a ZrO_2–SiO_2–B_2O_3 (BSZ) system was used for interpretation of the results. The convection cells formed during oxidation were fewer and less uniformly distributed for composites with a higher SiC concentration. This is because the convection cells are formed from ZrO_2 precipitates from a BSZ oxide liquid that forms upon oxidation of the composite at 1550°C. Higher SiC-containing composites will have less dissolved ZrO_2 because they have less B_2O_3, which results in a smaller amount of precipitated ZrO_2 and consequently fewer convection cells.

I. Introduction

The boride-based composites, ZrB_2–SiC and HfB_2–SiC, are considered among the most promising ceramic composites for high temperature and structural applications due to their unique properties.[1] The ZrB_2–SiC and HfB_2–SiC composites are ultra-high-temperature ceramics, that are oxidation resistant at high temperatures due to the presence of a complex multilayer oxide scale that slows down inward diffusion of the oxygen.[1–4] It is well known that SiC improves the oxidation behavior[4] by adding silica to the oxide film, but the details of the role of SiC in the amounts and compositions of the phases in the film have not been described in detail. This paper compares the oxide film microstructure after oxidation at 1550°C for three different SiC concentrations.

During high-temperature oxidation (>1200°C) of the ZrB_2–SiC composite, a liquid oxide film, borosilicate (SiO_2–B_2O_3), forms on the outer surface.[5,6] Solid zirconium oxide (ZrO_2) is also formed along with the liquid oxide film above the unreacted ZrB_2–SiC material. Because of the high vapor pressure of boria ($B_2O_3(l)$) at these temperatures, compared with silica ($SiO_2(l)$), the B_2O_3 is preferentially evaporated from the borosilicate liquid. The liquid oxide film at the outer surface then becomes a predominantly viscous SiO_2-rich borosilicate liquid.[1,2,7–9]

A novel oxidation mechanism involving flow of the liquid oxide has been proposed.[10] Flow of a boria–silica–zirconia (ZrO_2–SiO_2–B_2O_3 (BSZ)) liquid was used to explain the distinctive microstructural features on the external oxide surface and in cross section.[11] These features, called convection cells, consist of ZrO_2 "islands" located in larger SiO_2-rich "lagoons" with B_2O_3-rich patterns surrounding the islands.[10–12] These features are shown in Fig. 1, which shows a surface of a ZrB_2-15 vol% SiC composite oxidized at 1600°C for 30 min. The area around the convection cells consists of a SiO_2-rich glass with small micrometer-sized zirconia dispersoids. The B_2O_3-rich flower petal-like patterns are visible in backscattered electron (BSE) imaging, and in stronger contrast in cathodoluminesence imaging, but are not observed in secondary electron imaging scanning electron microscopy (SEM). We previously suggested that ZrO_2 cores form by precipitation during the evaporation of boria (B_2O_3) from a BSZ liquid that rises through the outer SiO_2-rich borosilicate layer and flows laterally, forming the B_2O_3-rich regions (the petals) around the ZrO_2 islands.[10,11] The BSZ liquid is formed when a borosilicate liquid rich in B_2O_3 dissolves some ZrO_2. We estimate the compositions of these phases with the aid of a calculated isothermal section of a B_2O_3–SiO_2–ZrO_2 system at 1500°C to describe the equilibrium between a BSZ liquid and crystalline ZrO_2.[11] A distinction is made between two zirconia morphologies formed during oxidation. The "primary" zirconia (porous underlying $ZrO_2(s)$) is formed directly by the oxidation of ZrB_2 by oxygen diffusion through the SiO_2-rich borosilicate primary surface layer. The "secondary" zirconia is precipitated from the BSZ liquid. At the surface, the B_2O_3 evaporates from the BSZ liquid and secondary zirconia precipitates. The surface is then covered with the less volatile phases i.e. the silica-rich liquid and secondary zirconia, which are located near the site of the B_2O_3 evaporation (near the B_2O_3 petals). The secondary zirconia precipitates form the zirconia island and dispersed zirconia.[11] What we observe at room temperature are patterns of crystalline zirconia and glasses formed after the silicate liquid cools.[10–12]

The convection cell theory suggests that the formation of the convection cells is dependent on the composition of the BSZ liquid, which in turn is dependent on the composition of the ZrB_2–SiC composite. Here, three ZrB_2–SiC composites with

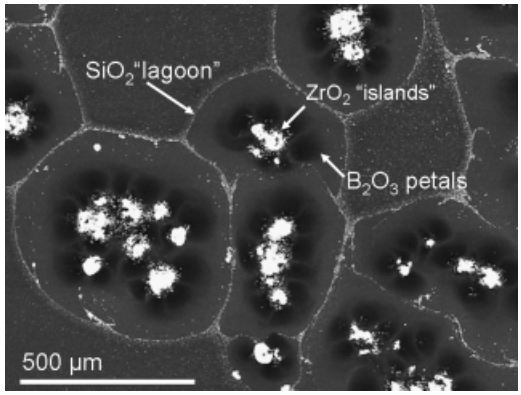

Fig. 1. Backscattering electron image of a surfaces of a ZrB_2-15 vol% SiC composite tested at 1600°C for $\frac{1}{2}$ h, showing an example of convection cells and their patterns.

M. Cinibulk—contributing editor

Manuscript No. 24488. Received March 31, 2008; approved November 5, 2008.
[‡]Current address is at the Department of Materials, Biotechnology and Energy, Innovation Center Iceland, IS-112 Reykjavik, Iceland.
[†]Author to whom correspondence should be addressed. e-mail: nanna@umich.edu

different SiC concentrations are tested at 1550°C for various durations of times and compared with study the effect of SiC concentration on the formation and distribution of convection cells.

II. Experimental Procedure

Three ZrB_2–SiC-based composites with different concentrations, 15, 20, and 30-vol% SiC, were used for this study. We presume that the decisive difference between the composites is their SiC concentration. These were provided by different laboratories and differed slightly in the processing, as described below. The ZrB_2-15 vol% SiC (ZS15) composite used for the study was provided and fabricated by Dr. Alida Bellosi and Dr. Frederic Monteverde at The Institute of Science and Technology for Ceramics, National Research Council (ISTEC-CNR) in Faenza, Italy. The properties and the processing of the ZS15 composite are presented in more detail elsewhere.[13] The ZrB_2 composites containing the 20% SiC and 30 vol% SiC were fabricated and provided by Dr. William G. Fahrenholtz, Dr. Gregory E. Hilmas, and associates at the University of Missouri-Rolla (UMR) in Rolla, MI. The ZrB_2-20 vol% SiC (ZS20) composite contained around 2 vol% WC that was incorporated in the attrition milling step during fabrication of the material at UMR due to the use of WC milling media. The fabrication and materials are described in more detail elsewhere.[14] The ZrB_2-30 vol% SiC (ZS30) composite was attrition milled at UMR with ZrO_2 milling media during fabrication; the presence of phases other than SiC and ZrB_2 was not reported, indicating no contamination from the milling media. The fabrication and starting materials are described in detail elsewhere.[15] Figure 2 shows the microstructure of the three composites ZS15, ZS20, and ZS30.

Oxidation was conducted in a high-temperature box furnace (SentroTech Corporation, Berea, OH) in ambient air at 1550°C at different dwelling times, ranging from 3 to 8 h. The heating and cooling rates used were 13°C/min. The three composites (ZS15, ZS20, and ZS30) were tested at 1550°C for 3, 4, and 8 h. The specimens were supported by sacrificial support pieces of the same ZS material. The sacrificial supports were placed on an Al_2O_3 support in an Al_2O_3 crucible. The ZS15 composite was cut into thin sheets from a bulk material with a wire electrical discharge machine (w-EDM) (Ann Arbor Machine Model 1S15, Ann Arbor, MI). The thin sheets of the ZS15 were then cut with a diamond saw (IsoMet® 1000 diamond precision saw, Buehler, Lake Bluff, IL) into small rectangular coupons with a total surface area between 0.5 and 1 cm^2. Then, ca. 200 μm was removed from the surface of the ZS15 coupons with a fine diamond grid (Omni Brade, TBW Industries, Furlong, PA) to remove any heat-affected zone that could have formed on the surface of the ZS15 sheets after the w-EDM. The ZS20 and ZS30 composites obtained from UMR as tests bars where ground and cut with the same tools as the ZS15 to obtain the same surface finish and a similar surface area (~0.5–1 cm^2) as the specimens tested. Before testing, the specimens were ultrasonically cleaned in acetone and dried at 100°C.

Microstructural analyses were performed on the surfaces and cross sections using SEM and BSE microscopy. The cross sections of the oxidized specimens were prepared for microstructural analysis by nonaqueous polishing procedures down to a 1 μm finish. Specimens were coated with carbon before the microstructural analysis.

III. Results: Microstructure Analysis

The purpose of testing other ZrB_2–SiC composites with different SiC concentrations was twofold: (1) to verify that convection cells form in ZrB_2–SiC materials other than the ZrB_2-15 vol% SiC (ZS15) composite previously studied by the authors[10–12,16] and (2) to study the effect of SiC concentration on the formation and distribution of convection cells. The evaluation of convection cells with time and temperature, formed at the oxide scale during high-temperature oxidation on the ZS15 composite, has been studied in detail and reported elsewhere.[16]

(1) Surface Analysis

Microstructure analysis with SEM and BSE imaging revealed that the ZS15, ZS20, and ZS30 specimens tested at 1550°C for 3, 4, and 8 h all showed the formation of convection cells on the surfaces. The convection cells on the ZS20 and ZS30 specimens were comparable to ZS15. However, the distribution and the number of cells formed on the surfaces of the three specimens were somewhat different from each other. Firstly, the ZS20 and ZS30 specimens had, in general, fewer convection cells than the ZS15 and they were not as uniform as the convection cells for the ZS15. Secondly, the ZS30 specimen tested at 1550°C for shorter dwelling times (3 and 4 h) had smaller ZrO_2 islands, sometimes surrounded by B_2O_3 circles instead of distinct petals. An example of this is shown in Fig. 3, where BSE images are shown of the surfaces of the three composites, ZS15, ZS20, and ZS30, tested at 1550°C for 4 h. The images were taken at low magnifications (× 36–38, 20 KV, spot size: 5) to be able to compare the population and the distribution of the convection cells on the three composites. The micrographs in Fig. 3 indicate that the lower SiC-containing composite (ZS15) has a larger number of convection cells spread over the surface than the higher SiC-containing composites (ZS20 and ZS30). To investigate this, the number of convection cells was quantified for the ZS15, ZS20, and ZS30 specimens by visual counting. The number of convection cells per square mm (cell density: no./mm^2) was quantified by counting the number of cells in a blinded fashion from 15 random fields (a square frame; 1 mm × 1 mm) per sample at × 36–38 microscopic magnification. The cell counts were then averaged for each sample. The quantification technique was based on protocols for manual quantification of biological features.[17,18] Figure 4 shows a graph of the average cell densities and the standard error (±standard deviation) for the three composites tested at 1550°C for 3, 4, and 8 h. The standard deviations (the error bars) of the values for the ZS20 and ZS30 composites are rather large, and the values for the 8-h oxidation time for the ZS20 and ZS30 do not differ much from ZS15. Overall, the results indicate that with increasing amount of SiC, fewer convection cells form. The large standard deviation for the ZS20 and ZS30 composites (in Fig. 4) was most likely because the convection cells on the ZS20 and ZS30

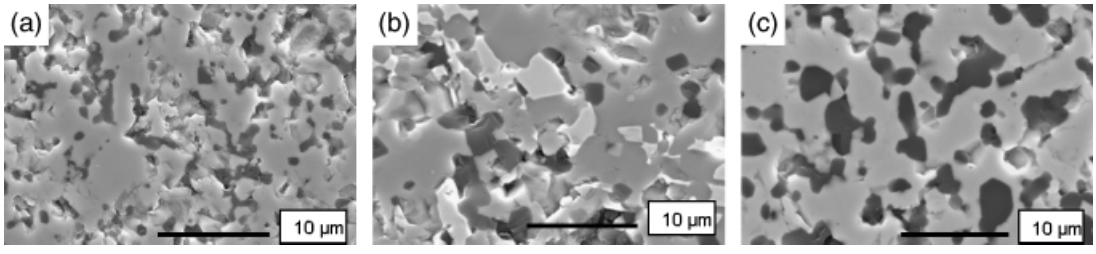

Fig. 2. Secondary electron images of the microstructure of the three different composites tested (a) ZrB_2-15 vol% SiC (ZS15), (b) ZrB_2-20 vol% SiC (ZS20), and (c) ZrB_2-30 vol% SiC (ZS30). The dark phases are the SiC grains and the light gray are the ZrB_2 grains, additionally the white phase for the ZS20 is reported elsewhere to be WC grains.[14]

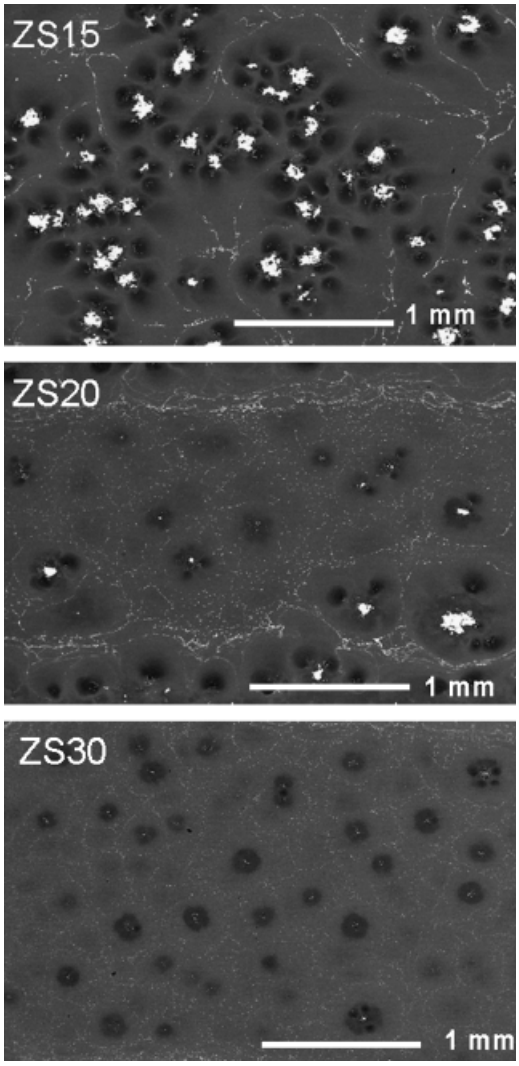

Fig. 3. Backscattering electron images of the surfaces of the ZrB_2 composites containing different amount of SiC; ZrB_2-15 vol% SiC (ZS15), ZrB_2-20 vol% SiC (ZS20), and (c) ZrB_2-30 vol% SiC (ZS30), all tested at 1550°C 4 h.

specimens were not uniformly distributed; thus, the cell density in one area differed from other areas. The decrease in the cell density in the ZS15 composite for the longer oxidation time at 1550°C, i.e. 8 h, can be seen in Fig. 4. It was previously shown that some convection cells may become "extinct" after they form and later become covered by fresh SiO_2 liquids depositing on the surface. Thus, the cell density decreases with longer oxidation time.[16]

In general, the features of the convection cells formed on the ZS20 and ZS30 are very similar to what was observed on the ZS15 specimens, i.e. ZrO_2 islands surrounded by B_2O_3-rich regions (petals) and outer SiO_2 lagoons. The similarity of the

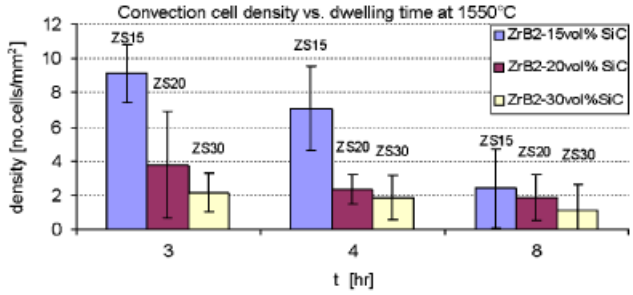

Fig. 4. The density of convection cells (no. cells/mm^2) for the three composites containing different amount of SiC; ZS15, ZS20, and ZS30 tested at 1550°C for 3, 4, and 8 h.

convection cells formed on the three composites is also indicated by ZrO_2 dendrites that were observed close to the ZrO_2 islands for all three composites. The formation of these dendrites is discussed in detail elsewhere.[16] An example of these dendrites on the ZS15, ZS20, and ZS30 composites is shown in Fig. 5, where BSE images of the surfaces of ZS15, ZS20, and ZS30, tested at 1550°C for 3, 3, and 8 h, respectively, are shown. The presence of dendritic zirconia adjacent to the islands is presented as evidence that the secondary zirconia is precipitating from a saturated liquid solution.

(2) Cross-Sectional Analysis

Figure 6 shows the secondary electron micrographs of cross sections of the ZS15, ZS20, and ZS30 specimens tested for 8 h. at 1550°C. The micrographs show enhanced oxidation zones (deeper recession) under the ZrO_2 islands where the cross sections cut through the convection cells. The contrast conditions for Fig. 6 do not clearly distinguish the interface between the oxide and the unreacted bulk, but these are shown clearly in backscattered imaging, and we indicate the interface using a broken line. The enhanced oxidation zones under the ZrO_2 islands of the convection cells are discussed elsewhere.[12] But, in summary, it forms when the BSZ liquid squeezes up to the surface and thus a path is open for more rapid inward diffusion of oxygen due to the lower viscosity of the BSZ liquid compared with the surrounding SiO_2-rich surface liquid layer.[12]

The thickness of the oxide layer for each composite increases with increasing dwelling time; this is shown in Fig. 7, which shows graphs of the total thickness of the oxide layer versus dwelling time at 1550°C for the three composites. The total oxide thickness was calculated as the sum of the measured averages of the SiO_2-rich borosilicate surface layer and the underlying ZrO_2 layer ($d_{avg} = d_{SiO_2rich} + d_{ZrO_2}$). The thickness of each layer was measured by averaging 20–30 values at various locations. A large standard deviation in the oxide thickness was found due to the deeper recession under the convection cells.

Fewer convection cells were found in the cross sections of the higher SiC-containing composites. This is in agreement with the surface analysis; there was fewer convection cells as the SiC content increased. From Figs. 6 and 7 it is evident that there is less oxidation for the higher SiC-containing composites. This is

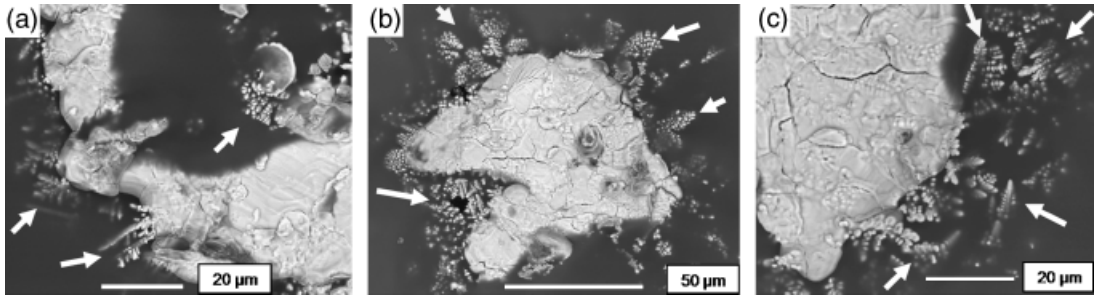

Fig. 5. Backscattering electron micrographs of a ZrO_2 islands on the surfaces (a) ZS15, (b) ZS20, and (c) ZS30 composites tested at 1550°C for 3 h (a), (b) and 8 h. (c), respectively, showing dendrites (indicated by arrows) grown close to the ZrO_2 islands.

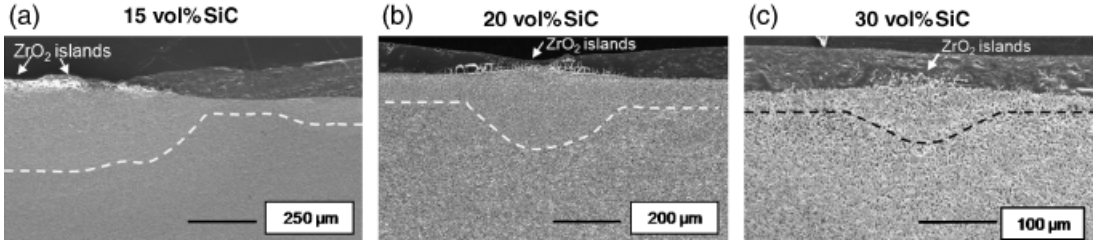

Fig. 6. Secondary electron micrographs of the cross-sections of (a) ZS15, (b) ZS20, and (c) ZS30 composites tested at 1550°C for 8 h. The interface between the ZrO_2 layer and the unreacted bulk material is indicated with a broken line. The darker outermost layer is the SiO_2-rich surface layer.

consistent with what has been published by Chamberlain *et al.*[14] on the ZrB_2-20 vol% SiC composite material and other ZrB_2–SiC composites with various SiC concentrations tested under similar oxidation conditions.

IV. Discussion and Phase Equilibrium Analysis

The results of the present study show that convection cells form, in general on ZrB_2–SiC composites during oxidation at higher temperatures (~1550°C). This supports the previous hypothesis[10,11] that the formation of the convection cells is dependent on the formation of a transient BSZ liquid and a large volume increase that occurs during oxidation of ZrB_2–SiC-based materials. Fewer convection cells (no. of cells/mm^2) form on a higher SiC-containing composite, i.e. ZS20 and ZS30, compared with ZS15, the lower SiC-containing composite. We suggest that this may be due to the difference in the composition of the BSZ liquid that forms during oxidation. The ZS20 and especially the ZS30 show less B_2O_3 (in the BSZ(l)) formation compared with the ZS15; thus, there should be less ZrO_2 dissolved in the BSZ liquid, which should result in formation of fewer ZrO_2 islands. This is supported by a calculated ternary phase diagram for the B_2O_3–SiO_2–ZrO_2 system at 1500°C published previously by the authors and Karlsdottir *et al.*,[11] and from the microstructural analysis and quantification of convection cells shown here.

The calculated ternary phase diagram for the B_2O_3–SiO_2–ZrO_2 system at 1550°C does not exist and so we have to use the only available ternary phase diagram for this system, which is a calculated phased diagram at 1500°C (the experimental diagram does not exist either). We justify this by pointing out that from a calculated binary phase diagram of the B_2O_3–ZrO_2 system,[11] the solubility of the zirconia would only be a slightly higher at 1550°C. Thus, we are not overestimating the amount of secondary zirconia. The authors do acknowledge that the calculated ternary phase diagram must be regarded as somewhat speculative. However, the general features of the system can be expected to be qualitatively correct. A detailed description of the calculation of the phase diagram is given elsewhere.[11] It should be stated here that although the calculated phase diagram can be used for the interpretation of the results, there is a strong need for experimental phase diagram for the ternary B_2O_3–SiO_2–ZrO_2 system, which, hopefully, future experimental investigations may provide.

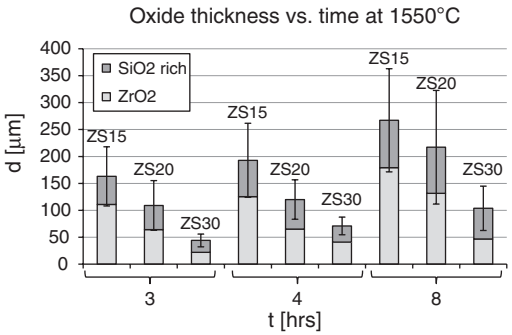

Fig. 7. The total oxide thickness of the ZS15, ZS20, and ZS30 composites tested at various dwelling times. Calculated by adding the measured thicknesses of the SiO_2—rich surface layer and the underlying ZrO_2 layer.

Figure 8 shows the isothermal section of the B_2O_3–SiO_2–ZrO_2 system at 1500°C, annotated on the lower right to show the equilibrium compositions expected for the fresh products of oxidation of zirconium diboride with 15, 20, or 30 vol% SiC. These oxide compositions fall in the two-phase region with the BSZ liquid solution and crystalline zirconia (ZrO_2). The phase diagram in Fig. 8 shows (indicated by arrows) how higher SiC-containing material would have a smaller amount of dissolved ZrO_2 in the BSZ liquid formed upon oxidation at 1500°C. This is because the B_2O_3 dissolves the ZrO_2 and SiO_2 but for higher SiC-containing composites, there is relatively less B_2O_3 and thus there will be less dissolved ZrO_2 in the BSZ liquid.[11] Annotations on the upper left portion of Fig. 8 also show the compositions expected after the B_2O_3 evaporates from the BSZ liquids (assuming 90% of the B_2O_3 has evaporated away as an example).

Consider the oxidation of a ZrB_2-15 vol% SiC composite at 1500°C. We expect the phase assemblage for the complete oxidation of the composite to be, on a molar basis, 0.33 mol solid ZrO_2 and 0.67 mol of a BSZ liquid (liquid composition 71 mole% B_2O_3+18 mol% SiO_2+11 mol% ZrO_2; this composition is indicated on the phase diagram with a white circle, see Fig. 8). At these temperatures, the $B_2O_3(l)$ will preferentially evaporate when the BSZ liquid reaches the surface and the dissolved ZrO_2 must precipitate out. If, for example, 90% of the $B_2O_3(l)$ evaporates away, assuming it stops due to increased viscosity when the relative amount of SiO_2 increases in the BSZ liquid and only 10% of B_2O_3 remains in the liquid, then there would be a shift towards the two-phase region in the phase diagram where ZrO_2 precipitates, and the final equilibrium phase assemblage would be a two-phase mixture, solid ZrO_2 (precipitated) and SiO_2-rich BSZ liquid, with the BSZ liquid composition being 88 mol% SiO_2, 2 mol% ZrO_2 and 10 mol% B_2O_3, and with the total composition changing to 58 mol% SiO_2, 36 mol% ZrO_2, and 6 mol% B_2O_3. The equilibrium phase assemblage at this composition is 66 mol% of a SiO_2-rich liquid and 34 mol% solid precipitated ZrO_2. The amount of ZrO_2 that will precipitate under these oxidation conditions for the higher SiC concentrated composites (ZS20 and ZS30) can be estimated in the same way as in the phase diagram, and is shown in Table I.

In Table I, the estimated amount of precipitated $ZrO_2(s)$ is shown for the three different ZrB_2–SiC composites. It also shows how the solubility of the $ZrO_2(s)$ in the BSZ liquid decreases with increasing viscosity and SiC concentration (i.e., increasing SiO_2 amount). The viscosity of the borosilicate melt was estimated from a relationship extrapolated from data by Jabra *et al.*[19] discussed in detail elsewhere.[10,11] The estimated amount of precipitated ZrO_2 decreases with increasing SiC content in the composites as shown in Table I. For example the ZrB_2-15 vol% SiC composite (ZS15) is estimated to precipitate 22 mol% more $ZrO_2(s)$ than the ZrB_2-30 vol% SiC (ZS30), when 90 mol% of the B_2O_3 has evaporated from the BSZ liquid. Less ZrO_2, precipitated from the BZS liquid, will result in fewer convection cells formed during oxidation; this could explain the decrease in the number of convection cell on the ZrB_2–SiC

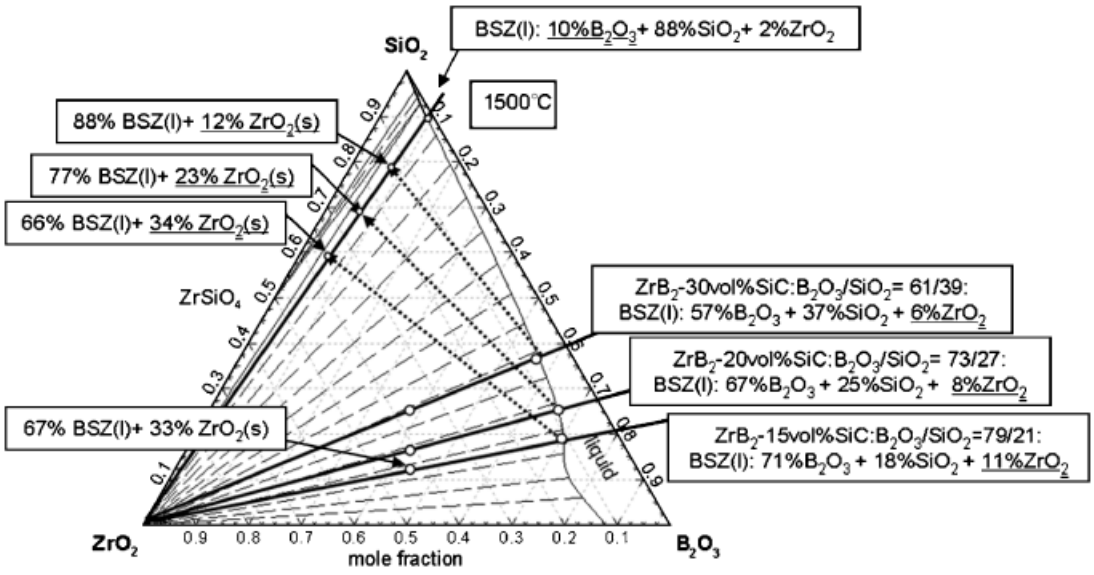

Fig. 8. Calculated ternary phase diagram of an isothermal section of the ZrO_2–SiO_2–B_2O_3 system at 1500°C.[11] The annotations in the lower right shows the equilibrium compositions expected for the fresh products of oxidation of zirconium diboride with 15, 20, or 30 vol% SiC and in the upper left shows the compositions anticipated after the B_2O_3 evaporates from the BSZ liquids.

composites with a higher SiC concentration, as on the ZS20 and ZS30 composites compared with the ZS15 composite.

The cross-sectional analysis for all three composites showed that a larger content of SiC yields a more oxidation-resistant composite, indicated by the decrease in total oxide scale thickness with increasing SiC content. The increased oxidation resistance of the higher SiC-containing materials could be explained by the composition of the BSZ liquid phase. With more SiC in the composite, there is less B_2O_3 content in the BSZ liquid. With less B_2O_3, the liquid is more viscous so that oxygen diffusion through the liquid is slower, which would result in less inward oxygen diffusion through the middle of the cell where the BSZ liquid squeezes out (SiO_2-rich BSZ liquid retards inward oxygen diffusion better than B_2O_3-rich liquid). Also, higher SiC-containing material will form a SiO_2-rich surface layer quicker than a lower SiC-containing material, thus hindering oxygen diffusion inward towards the bulk material sooner and thus more effectively. Also, if a SiO_2-rich surface layer is formed faster, then it can suppress the evaporation of the B_2O_3 and a protective surface layer can be formed quicker.

V. Conclusions

ZrB_2–SiC composites with 20 and 30 vol% SiC oxidized at 1550°C show convection cell features similar to convection cells formed on an oxidized ZrB_2-15 vol% SiC composite. Convection cell density decreases with increased oxidation time and SiC concentration in ZrB_2–SiC composites. The effect of SiC concentration on convection cell density can be correlated to the liquid and solid-phase assemblage where composites with more SiC have BSZ liquid with a larger SiO_2/B_2O_3 ratio, which dissolves less ZrO_2, and thus results in a smaller cell density. The influence of SiC content on the oxidation rate of ZrB_2–SiC composites can be understood in terms of the composition and amount of BSZ liquid.

Table I. The Amount of Precipitated Secondary ZrO_2(*s*); BSZ Liquid Composition; and Estimated Viscosity,[10,11] for the Three ZrB_2–SiC Composites Estimated by Using the ZrO_2–B_2O_3–SiO_2 Ternary Phase Diagram Shown in Fig. 8

SiC concentration (mol%)	BSZ composition ZrO_2, SiO_2, B_2O_2 (mol%)	Precipitated ZrO_2(S) (mol% of total composition)	Estimated viscosity (Pa · s)
15	11, 18, 71	34	6.3×10^2
20	8, 25, 67	23	5.0×10^3
30	6, 37, 57	12	3.9×10^4

BSZ, ZrO_2–SiO_2–B_2O_3.

Acknowledgments

We thank Dr. David Shifler of the Office of Naval Research for supporting the research under contract N00014-02-1-0034, and Drs. Alida Bellosi, Frederick Monteverde, Gregory Hilmas, and William Farhenholtz for providing the ZrB_2–SiC composites used for this study and valuable discussions.

References

[1]M. M. Opeka, I. G. Talmy, and J. A. Zaykoski, "Oxidation-Based Materials Selection for 2000°C+Hypersonic Aerosurface: Theoretical Considerations and Historical Experience," *J. Mater. Sci.*, **39** [19] 5887–904 (2004).

[2]M. M. Opeka, I. G. Talmy, E. J. Wuchina, J. A. Zaykoski, and S. J. Causey, "Mechanical, Thermal, and Oxidation Properties of Refractory Hafnium and Zirconium Compounds," *J. Eur. Ceram. Soc.*, **19**, 2405–14 (1999).

[3]R. Telle, L. S. Sigl, and K. Takagi, "Transition Metal Boride Ceramics"; pp. 803–945 in *Handbook of Ceramic Hard Materials*, Vol. 2, Edited by R. Reidel. Wiley-VCH, Weinheim, Germany, 2000.

[4]W. C. Tripp, H. H. Davis, and H. C. Graham, "Effect of SiC Addition on the Oxidation of ZrB," *Am. Ceram. Soc. Bull.*, **52** [8] 612–6 (1973).

[5]R. A. Cutler, "Engineering Properties of Borides"; pp. 787–803 in *Ceramics and Glasses, Engineering Materials Handbook*, Vol. 4, Edited by S. J. Schneider. ASM International, Materials Park, OH, 1992.

[6]S. R. Levine, E. J. Opila, M. C. Halbig, J. D. Kiser, M. Singh, and J. A. Salem, "Evaluation of Ultra-High Temperature Ceramics for Aeropropulsion Use," *J. Eur. Ceram. Soc.*, **22**, 2757–67 (2002).

[7]F. Monteverde and A Bellosi, "Oxidation of ZrB_2-Based Ceramics in Dry Air," *J. Electrochem. Soc.*, **150** [11] B-552–9 (2003).

[8]W. G. Fahrenholtz, "The ZrB_2 Volatility Diagram," *J. Am. Ceram. Soc.*, **88** [12] 3509–12 (2005).

[9]W. G. Fahrenholtz, "Thermodynamics of ZrB_2–SiC Oxidation: The Formation of a SiC-Depleted Region," *J. Am. Ceram. Soc.*, **90** [1] 142–8 (2007).

[10]S. N. Karlsdottir, J. W. Halloran, and C. E. Henderson, "Convection Patterns in Liquid Oxide Films on ZrB_2–SiC Composites Oxidized at a High Temperature," *J. Am. Ceram. Soc.*, **90** [9] 2863–7 (2007).

[11]S. N. Karlsdottir, J. W. Halloran, and A. N. Grundy, "Zirconia Transport by Liquid Convection During Oxidation of Zirconium Diboride-Silicon Carbide Composite," *J. Am. Ceram. Soc.*, **91** [1] 272–7 (2008).

[12]S. N. Karlsdottir and J. W. Halloran, "Formation of Oxide Films on ZrB_2–SiC Composites During Oxidation: Relation of Subscale Recession to Liquid Oxide Flow," *J. Am. Ceram. Soc.*, **91** [11] 3652–8 (2008).

[13]S. N. Karlsdottir, J. W. Halloran, F. Monteverde, and A. Bellosi, "Oxidation of ZrB_2–SiC: Comparison of Furnace Heated Coupons and Self-Heated Ribbon Specimens"; *Proceedings of the International Conference on Advanced Ceramics and Composites,* Daytona Beach FL, January 21–26, (2007).

[14]Chamberlain, W. Fahrenholtz, G. Hilmas, and D. Ellerby, "Oxidation of ZrB_2–SiC Ceramics under Atmospheric and Reentry Conditions," *Refractories Appl. Trans.*, **1** [2] 1–8 (2005).

[15]A. Rezaie, W. G. Fahrenholtz, and G. E. Hilmas, "Oxidation of Zirconium Diboride–Silicon Carbide at 1500°C at a Low Partial Pressure of Oxygen," *J. Am. Ceram. Soc.*, **89** [10] 3240–5 (2006).

[16]S. N. Karlsdottir and J. W. Halloran, "Formation of Oxide Films on ZrB_2–SiC Composites During Oxidation: Evolution with Time and Temperature," *J. Am. Ceram. Soc.*, 2008, (accepted).

[17]A. Wackernagel, C. Massone, G. Hoefler, E. Steinbauer, H. Kerl, and P. Wolf, "Plasmacytoid Dendritic Cells are Absent in Skin Lesions of Polymorphic Light Eruption," *Photodermatol., Photoimmunol. Photomed.*, **23**, 24–8 (2007).

[18]H. Daims and M Wagner, "Quantification of Uncultured Microorganisms by Fluorescence Microscopy and Digital Image Analysis," *Appl. Microbiol. Biotechnol.*, **75**, 237–48 (2007).

[19]R. Jabra, J. Phalippau, and J. Zarzicki, "Synthesis of Binary Glass-Forming Oxide Glasses by Hot-Pressing," *J. Non-crystalline Solids*, **42**, 489–98 (1980). □